A MAGNETICALLY SWITCHED TRIGGER SOURCE FOR FXR*

H. C. Kirbie, G. Y. Otani, and G. M. Hughes
Lawrence Livermore National Laboratory
Livermore, California 94550

Abstract

This paper describes the design and performance of a three-stage magnetic pulse compressor used to trigger the Flash X-Ray Accelerator at Lawrence Livermore National Laboratory. Each of two compressors generates a pulse onto a bundle of thirteen parallel cables. The cables carry the pulse to a network of spark gaps that initiates the accelerator charge and discharge sequence. The performance data illustrate the compression of a 7.7-μs, dual-resonant waveform into a 232-ns (FWHM) unipolar pulse with an 80-ns risetime and a maximum *dV/dt* of 1.98 kV/ns. Additional data are also presented to show network jitter, efficiency, and sensitivity to small changes in charge voltage and reset current.

Introduction

The Lawrence Livermore National Laboratory Flash X-Ray (FXR) Accelerator generates a single, intense burst of x rays by focusing a 50-ns beam of 18-MeV electrons onto a small tungsten target.[1] The flash of x rays is used to diagnose the hydrodynamic behavior of a chemical explosion by taking an x-ray snapshot of the event at a specific moment in time. Since the accelerator was designed for single-shot duty, the pulsed power system uses spark gaps to switch 13 Marx banks, which in turn charge 54 water-filled Blumlein transmission lines. Each Blumlein line has a single spark gap attached to one end and a ferrite-loaded accelerator cell attached to the other end. When the Blumlein spark gap is triggered, a 90-ns voltage pulse is produced at the cell.

The FXR trigger system, shown in Fig. 1, is based on a low-maintenance magnetic pulse compressor. The design replaced the original FXR trigger system,[2] which was very effective but which required constant maintenance as it aged. Eventually, the maintenance effort could no longer assure that the original system would produce a pulse within acceptable jitter limits. The new system uses two magnetic compressors initiated by spark gaps to generate a 100-kV, 1.9-GW, fast-rising pulse onto two bundles of thirteen 67.6-Ω cables. Like its predecessor, the upgraded trigger system is fully redundant because each compressor uses two spark gaps to help ensure that an input pulse will be initiated. The magnetic switching network, being passive, is a very reliable pulse compression system.

The system described in this paper is similar in design to one described by Birx[3] in which a three-stage magnetic compressor pulses a bundle of trigger cables. However, the FXR compressor differs from Ref. 3 in its use of a dual-resonant transformer[4,5] that steps up the initial charge voltage and greatly reduces the voltage-dependent jitter of the circuit.

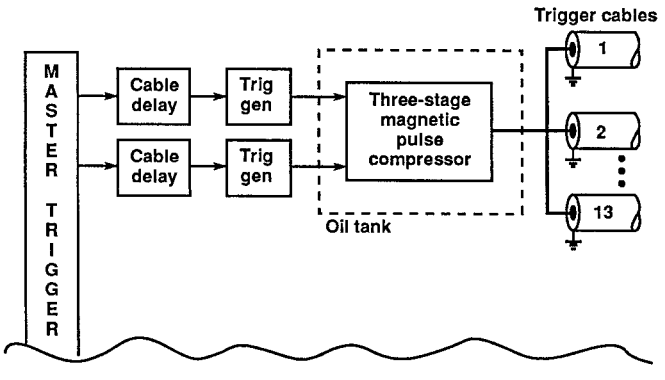

Figure 1. One half of the magnetically switched trigger system for the LLNL Flash X-Ray (FXR) accelerator. The system includes a duplicate of the network shown above.

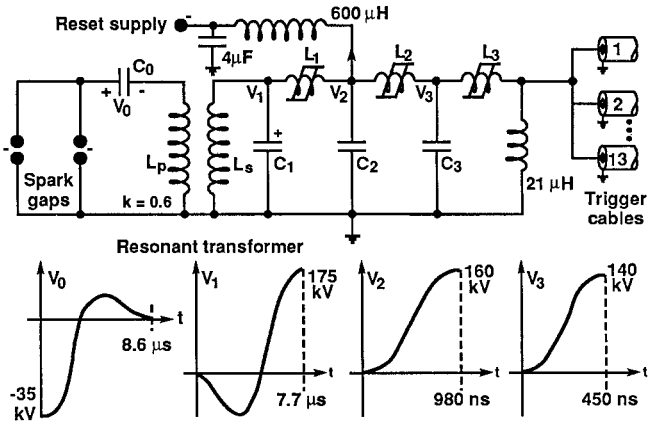

Figure 2. Simplified network diagram of the magnetic pulse compressor with voltage waveforms.

Network Design

Figure 2 is a circuit diagram of the magnetic pulse compressor. A dc power supply initially charges capacitor C_0 to +35 kV. The pulse is initiated by closing one of the two spark gaps that connects C_0 to the primary of a dual-resonant transformer. The transformer steps up the pulsed voltage to 175 kV on C_1. The first magnetic switch, L_1, saturates as the voltage peaks on C_1 and permits current from C_1 to charge C_2 to approximately 160 kV. Similarly, the second magnetic switch, L_2, saturates as the voltage peaks on C_2, which charges C_3 from C_2 to approximately 140 kV. When C_3 is fully charged, the last magnetic switch, L_3, saturates and connects C_3 to the cable bundle. The magnetically switched section of the circuit, from C_1 to the load, is known as a Melville or series pulse-compression line. A number of articles describe the design and operation of the Melville line in great detail.[6–8]

The air-core, dual-resonant transformer in Fig. 2 is designed to step up the available power supply voltage to 175 kV in a 600-J pulse. The energy and voltage levels were selected to endure the hysteretic and resistive circuit losses and still produce the desired pulse of 100 kV at the output. The 175-kV voltage at the transformer secondary is also the voltage on C_1 and is given by Eq. (1) when circuit resistance is neglected[4]:

$$V_1(t) = \frac{V_0}{2}\sqrt{\frac{L_s}{L_p}}\left[\cos\frac{\omega t}{\sqrt{1-k}} - \cos\frac{\omega t}{\sqrt{1+k}}\right], \qquad (1)$$

where V_0 = 35 kV, L_s = 111.7 μH, L_p = 3.0 μH, ω = 480 krad/s, and the coupling coefficient, k, is 0.6.

The complex waveform described by Eq. (1) removes the voltage-dependent jitter from the first-stage switch, L_1. The flux density in the core of L_1 builds up to saturation as the integral of the applied voltage. Figure 3 shows the voltage on C_1 and the flux density in L_1 as a function of time. Ideally, the voltage on C_1 is integrally symmetric because the negative and positive portions of the voltage wave have the same volt-second content. As a result, switch L_1 has a flux density that begins and ends at the same saturated level. The dashed lines of Fig. 3, representing an arbitrary increase in charge voltage, illustrate the advantage gained by the resonant waveform of Eq. (1). Even though the resonant wave becomes bigger, it still remains integrally symmetric and caused L_1 to saturate at the same moment. Therefore, the switching action of L_1 always occurs at the peak voltage of C_1 without regard to small changes in the charge voltage. The remaining two magnetic switches, L_2 and L_3, still exhibit a voltage-dependent jitter, but their contribution is very small.

Report Documentation Page

Form Approved
OMB No. 0704-0188

1. REPORT DATE	2. REPORT TYPE	3. DATES COVERED
JUN 1989	**N/A**	**-**

4. TITLE AND SUBTITLE	5a. CONTRACT NUMBER
A Magnetically Switched Trigger Source For Fxr	5b. GRANT NUMBER
	5c. PROGRAM ELEMENT NUMBER
6. AUTHOR(S)	5d. PROJECT NUMBER
	5e. TASK NUMBER
	5f. WORK UNIT NUMBER
7. PERFORMING ORGANIZATION NAME(S) AND ADDRESS(ES) **Lawrence Livermore National Laboratory Livermore, California 94550**	8. PERFORMING ORGANIZATION REPORT NUMBER
9. SPONSORING/MONITORING AGENCY NAME(S) AND ADDRESS(ES)	10. SPONSOR/MONITOR'S ACRONYM(S)
	11. SPONSOR/MONITOR'S REPORT NUMBER(S)

12. DISTRIBUTION/AVAILABILITY STATEMENT
Approved for public release, distribution unlimited

13. SUPPLEMENTARY NOTES
See also ADM002371. 2013 IEEE Pulsed Power Conference, Digest of Technical Papers 1976-2013, and Abstracts of the 2013 IEEE International Conference on Plasma Science. Held in San Francisco, CA on 16-21 June 2013. U.S. Government or Federal Purpose Rights License.

14. ABSTRACT
This paper describes the design and performance of a three-stage magnetic pulse compressor used to trigger the Flash X-Ray Accelerator at Lawrence Livermore National Laboratory. Each of two compressors generates a pulse onto a bundle of thirteen parallel cables. The cables carry the pulse to a network of spark gaps that initiates the accelerator charge and discharge sequence. The performance data illustrate the compression of a 7.7-Jls, dual-resonant waveform into a 232-ns (FWHM) unipolar pulse with an 80-ns risetime and a maximum dV/dt of 1.98 kV /ns. Additional data are also presented to show network jitter, efficiency, and sensitivity to small changes in charge voltage and reset current.

15. SUBJECT TERMS

16. SECURITY CLASSIFICATION OF:			17. LIMITATION OF ABSTRACT	18. NUMBER OF PAGES	19a. NAME OF RESPONSIBLE PERSON
a. REPORT	b. ABSTRACT	c. THIS PAGE			
unclassified	**unclassified**	**unclassified**	**SAR**	**4**	

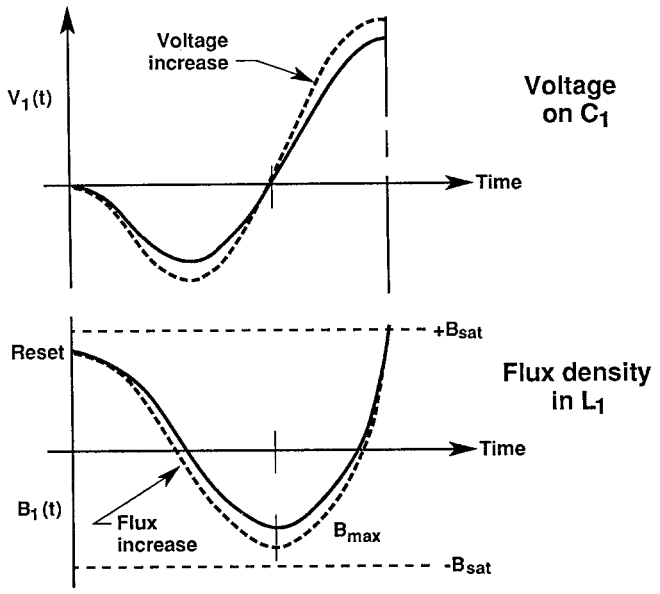

Figure 3. Sketch of the voltage at C_1 and the resulting flux density (B_1) in L_1. Dashed lines indicate the effects of a charge voltage increase.

Each of the three magnetic switches contains a core of 2605CO Metglas tape wound with Mylar film for insulation. The first magnetic switch (L_1) is sized so that B_{max} would be less than B_{sat} for the peak operating voltage (see Fig. 3). The value of B_{max} is given by

$$B_{max} = \frac{1}{N_1 A_1} \int_0^{0.843\pi/\omega} V_1(t)\, dt \ , \qquad (2)$$

where N_1 is the number of turns on L_1, A_1 is the magnetic cross-sectional area, and $V_1(t)$ is given by Eq. (1). The evaluation of Eq. (2) yields an expression for B_{max}:

$$B_{max} = \frac{V_1(\text{max})\ 1.6432}{2\omega N_1 A_1} \leq 3\ \text{T} \ , \qquad (3)$$

where ω = 480 krad/s and V_1(max) = 175 kV. In this case, L_1 was designed with a flux swing of B_{max} = 3 T by selecting N_1 = 9 turns and A_1 = 11.13 × 10^{-3} m^2. A peak voltage greater than 175 kV will saturate L_1 slightly at B_{max}. This condition is favorable because it generates an early current pulse that is oriented to reset L_2 and L_3 before the main pulse arrives. Once fully saturated, the inductance of L_1 drops to 4.1 μH. The combination of L_1 and structure inductance allows C_2 to charge in 980 ns.

The voltages on C_2 and C_3 are each unipolar and rise with a 1 – cos ωt waveshape. Switches L_2 and L_3 are sized to saturate when the voltage peaks on each preceding capacitor. When fully saturated, each switch transfers the energy to the next stage through the stray inductance of the structure.

Table 1 is an electrical and mechanical summary of each magnetic compression stage. The drop in charge voltage from C_1 to C_2 and from C_2 to C_3 is caused by a combination of resistive and magnetic losses encountered by the pulse at each stage of compression. In addition, the saturation times of L_2 and L_3 were adjusted to slightly exceed the charge times of C_2 and C_3. This was done to allow some increase in input voltage and still have L_2 and L_3 switch on the voltage peaks.

Capacitor C_0 (Fig. 2) is a parallel combination of two 0.7-μF, 50-kV plastic case capacitors. The measured capacitance of C_0 is 1.40 μF with an estimated internal resistance of 70 mΩ. Capacitor banks C_1 and C_2 each contain four capacitors with a nominal value of 40 nF at 100 kV. The bank is configured by connecting two capacitors in series and joining that series branch in parallel with another. The resulting capacitor banks (C_1 = 39.2 nF and C_2 = 38.1 nF) have a 200-kV maximum charge voltage and an estimated internal resistance of 350 mΩ. The third capacitor bank, C_3, also contains four 40-nF capacitors but is configured to feed the last magnetic switch from two sides for low inductance. Each half of the C_3 bank is fitted with a current probe to compare the current contributions from each side.

The three magnetic switches must be reset (remagnetized) between pulses so that the cores will be ready to undergo a full flux reversal on the next pulse. This is achieved by passing a 15-A dc current through the switches in a direction that will reset the cores. The low-voltage dc power supply is protected from the high-voltage pulse by a large series inductor (600 μH) and shunt capacitor (4 μF), as shown in Fig. 2. The reset current flows to ground through two parallel paths of equal resistance. One path is through L_1 and the secondary winding of the resonant transformer. The other path is through L_2, L_3, and the 21-μH inductor connected across the output. The dc current must be well regulated to avoid reset variations appearing as jitter on the output pulse.

Table 1. Summary of switch parameters, dimensions, and component values for the three magnetic compression stages.

Stage data	Compression stage		
	First (L_1, C_1)	Second (L_2, C_2)	Third (L_3, C_3)
Magnetic material (thickness)	2605CO (25.4 μm)	2605CO (25.4 μm)	2605CO (25.4 μm)
Core insulation (thickness)	Mylar (7.6 μm)	Mylar (12.7 μm)	Mylar (12.7 μm)
Number of core laminations	2875	2700	2350
Number of core sections (height)	3 (50.8 mm)	3 (50.8 mm)	5 (50.8 mm)
Magnetic cross section	11.13 × 10^{-3} m^2	10.45 × 10^{-3} m^2	15.16 × 10^{-3} m^2
Average magnetic path length	0.810 m	0.838 m	0.791 m
Magnetic core volume	9.02 × 10^{-3} m^3	8.76 × 10^{-3} m^3	12.0 × 10^{-3} m^3
Magnetic losses/m^3	900 + 1500 J/m^3	3700 J/m^3	6700 J/m^3
Total magnetic core loss	21.64 J	32.4 J	80.4 J
Number of switch turns	9	3	1
Number of coil groups	4	12	1
Unsaturated permeability	4500 μ_0	1000 μ_0	550 μ_0
Unsaturated inductance	6.29 mH	141.1 μH	13.24 μH
Coil cross section	32.6 × 10^{-3} m^2	32.6 × 10^{-3} m^2	46.0 × 10^{-3} m^2
Saturated inductance	4.1 μH	440 nH	70 nH
Bank capacitance, C_n	39.2 nF	38.1 nF	38.1 nF
Charge time of C_n	8.6 μs	980 ns	450 ns
Saturation time of L_n	7.7 μs	1.06 μs	525 ns
Stage gain	8.78	2.18	2.20
Gross switch weight	81.6 kg	81.6 kg	131.5 kg

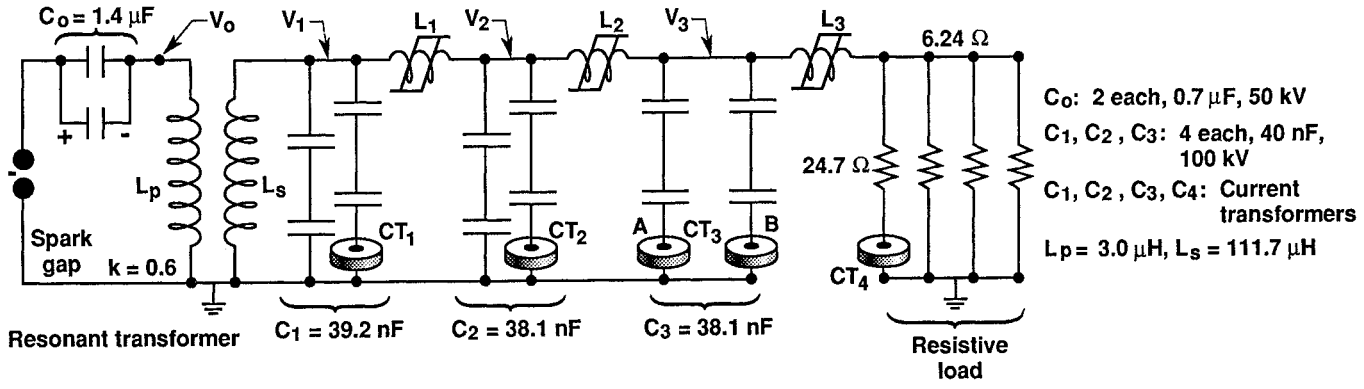

Figure 4. Detailed network diagram of the magnetic pulse compressor showing the resistive test load and current transformer locations.

Circuit Performance

The circuit of Fig. 2 was tested before installation by replacing the cable bundle with four ceramic resistors, as shown in Fig. 4. The parallel combination of resistors equals 6.24 Ω, which is 16.7% larger than the expected bundle impedance of 5.2 Ω. One of the four resistors measures 24.7 Ω and is fitted with a current transformer (CT_4) to estimate the output voltage.

Figure 5(a) shows the primary and secondary voltages of the resonant transformer. The primary voltage begins at –35 kV and reaches a second voltage zero in 8.6 μs. The secondary voltage (V_1) reaches a second peak of +175 kV in 7.7 μs. Figure 5(b) shows the voltage V_1 along with the current through CT_1. Capacitor C_1 is charged with a bipolar current that is near zero when L_1 saturates. The discharge of C_1 into C_2 yields a total peak current of 9.8 kA, which charges C_2 in 980 ns.

Figure 6(a) is a measure of the voltage on C_2 and the current through CT_2. In this case, the negative current signal charges C_2 to 160 kV and is equal to the large positive-current pulse of Fig. 5(b). Switch L_2 saturates in 1.06 μs and discharges C_2 into C_3 with a total peak current of 19.25 kA. Figure 6(b) shows the charging of each half of C_3 by the current probes CT_3 A and B. One of the two probes is inverted so that an analog subtraction of the two signals will indicate any power-flow imbalance. The total peak current and 450-ns charge time are used to estimate a 140-kV peak voltage on C_3. The discharge of C_3 is also indicated in Fig. 6(b) and the signals show a 17% peak imbalance between between the A and B discharge contributions.

Figure 7(a) shows the measured current through one of the four load resistors. The current monitor (CT_4) indicates a peak value of 4.4 kA, which implies an output voltage of 108.7 kV. The output pulse reaches a peak power of 1.9 GW and contains approximately 373 J of energy. The pulse rises in 80 ns (10–90%) with a maximum *dV/dt* of 1.98 kV/ns and an average *dV/dt* of 740 V/ns. In addition, the pulse width is 232 ns (FWHM) with a 10-kV prepulse.

Figure 7(b) shows the output pulse into a cable bundle using the same probe (CT_4) to monitor the current into a single 67.6-Ω cable. In this case, the cable current peaks at 1.4 kA, which implies a peak cable voltage of 94.6 kV. The negative reflection shown in the photograph arises from the open-circuit trigger electrode that is capacitively coupled to the cable. The short-lived open circuit causes the trigger voltage to double until the spark gap closes. Once closed, the coupling network appears as a matched cable load and suppresses further reflections.

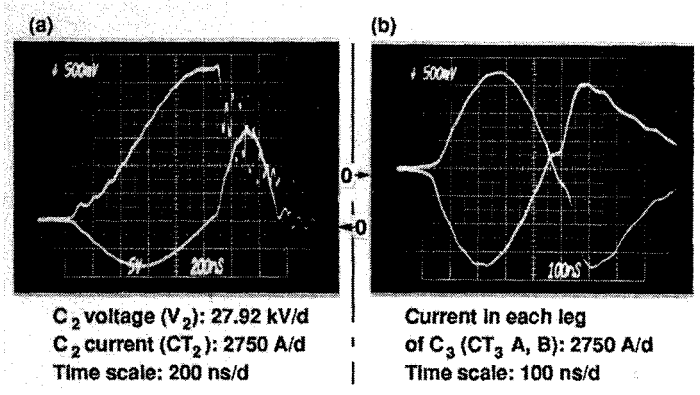

Figure 6. (a) Voltage and current waveforms for capacitor C_2. (b) Current in each leg of capacitor bank, C_3.

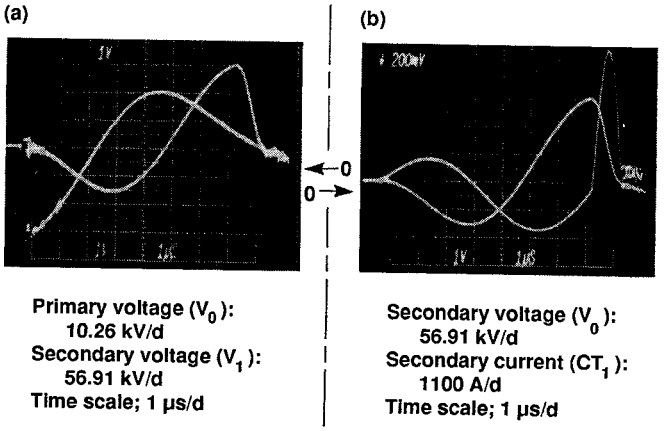

Figure 5. (a) Primary and secondary voltages on the resonant transformer. (b) Secondary voltage and current out of the resonant transformer.

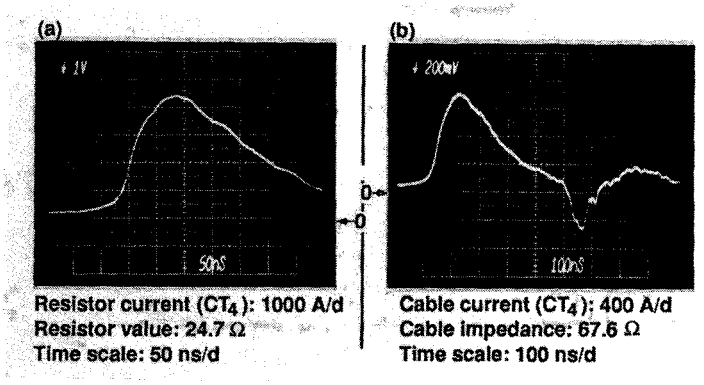

Figure 7. (a) Output waveform into the resistive test load. (b) Output waveform into a cable bundle on FXR.

The photographs of Fig. 8 illustrate the overall sensitivity of the compressor to independent changes in dc reset current and input charge voltage. Figure 8(a) shows a shift in the output pulse timing when reset current varies; the input voltage is held constant at 32.5 kV. Figure 8(b) shows a larger shift in output pulse timing arising from a variation in the input charge voltage with the reset current held constant at 20 A. Calculations indicate that the sensitivity of the compressor to charge voltage is dominated by the second-stage magnetic switch.

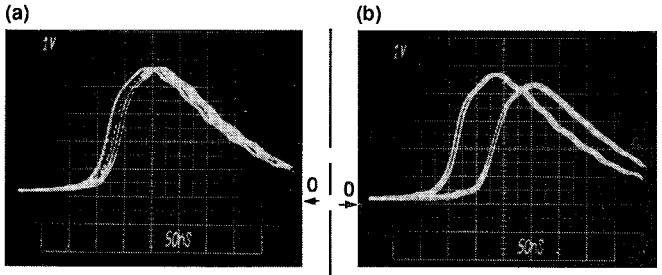

Figure 8. (a) Output pulse timing vs reset current. (b) Output pulse timing vs charge voltage.

The Melville section of the pulse compressor has an energy efficiency of 62.2%, as measured at C_1 and C_3. However, the overall efficiency from C_0 to C_3 is only 43.67%. The efficiency loss occurs because the resonant transformer is improperly tuned, which causes L_1 to switch 800 ns early. In doing so, a significant amount of energy becomes trapped in the primary circuit, where it cannot contribute to the output pulse.

Mechanical Design Details

The magnetic pulse compressor is an open-frame, oil-immersed machine built on a single aluminum base plate; the device measures 147.3 × 71.12 cm, and stands 137.2 cm high. The open-frame design simplifies machine maintenance and allows the entire 750-kg structure to be raised and lowered into an oil tank. Low electrical inductance is achieved by encircling the magnetic switches with a cage of twelve brass rods that conduct the pulsed currents and serve as structural members. The magnetic switches stack on top of one another with L_1 at the bottom.

The air-core transformer consists of two concentric solenoids with radii chosen to yield a coupling coefficient of 0.6. The primary solenoid is a four-turn spiral consisting of a copper foil insulated by four combined layers of Mylar and Kraft paper. The secondary solenoid, of similar construction, is a 32-turn spiral consisting of a copper foil insulated by two strips of Mylar film separated by a single layer of Kraft paper. The primary winding package has an average electric field strength of 131.2 kV/cm at 40 kV, while the secondary winding package has an average field strength of 109.4 kV/cm at 200 kV. The fields of both the primary and secondary coil structures are graded by split corona rings, similar to those described by Rohwein.[5] Additional voltage grading structures are provided by surfaces of electrically conductive plastic.

The first magnetic switch core is wound in three sections using 50.8-mm-wide, 2605CO Metglas alloy insulated with Mylar film. The core is encircled with four coils, each having nine turns and wound with the center conductor of RG-213/U coaxial cable. Each coil group terminates into two 41.9-cm-o.d. stainless steel electrodes mounted above and below the core. The second magnetic switch core also consists of three sections of 50.8-mm-wide, 2605CO Metglas alloy insulated with a Mylar film. In this case, the core is encircled with twelve coils, each having three turns of RG-213/U wire and terminated into two stainless-steel electrode plates. The third magnetic switch has two cores: one containing three 50.8-mm-high sections and the other containing two sections. Each core is wound around a section of aluminum pipe, which also carries the single-turn switch current. The taller, three-section core is fitted with a ring that receives the output trigger cables.

Summary

The previous trigger system for FXR has been replaced with two magnetic pulse compressors, each capable of generating a 100-kV pulse onto a bundle of thirteen 67.6-Ω cables. Both compressors have been in operation for two years at the FXR facility. In that time, the trigger system has been very reliable with a consistently high performance and a very low maintenance record.

Acknowledgments

Special recognition goes to Ron Hoard, Bill Denhoy, and Ed Folsom for their mechanical analysis of the machine's structure, material compatibility, and magnetic forces. The outstanding craftsmanship of the following MFD and NEED technical support personnel was also appreciated: Joe Farrington, Wayne Jensen, Bob Kuklo, Lisa Lauderbach, Dave O'Conner, Richard Parker, and Mike Wagoner. The Bunker 801 staff is also recognized for their diligent work in replacing the old trigger system with the new one. In this effort, Bill Edwards, Tony Ferriera, and Denise Kuklo each provided an essential contribution.

References

[1] B. Kulke, T. G. Innes, R. Kihara, and R. D. Scarpetti, "Initial Performance Parameters on FXR," in Proceedings of the Fifteenth IEEE Power Modulator Symposium, Baltimore, Maryland, 1982, p. 307.

[2] R. D. Scarpetti and C. D. Parkinson, "Switching System for the FXR Accelerator," in Proceedings of the Fourteenth IEEE Power Modulator Symposium, Orlando, Florida, 1980, p. 12.

[3] D. L. Birx, E. J. Lauer, L. L. Reginato, D. Rogers Jr., M. W. Smith, and T. Zimmerman, "Experiments in Magnetic Switching," in Proceedings of the Third IEEE Pulsed Power Conference, Albuquerque New Mexico, 1981, p. 262.

[4] E. G. Cook and L. L. Reginato, "Off-Resonance Transformer Charging for 250 kV Water Blumlein," IEEE Trans. Electron Devices, vol. ED-26, p.1512, October 1979.

[5] G. J. Rohwein, "Design of Pulse Transformers for PFL Charging," in Proceedings of the Second IEEE Pulsed Power Conference, Lubbock, Texas, 1979, p.87.

[6] W. S. Melville, "The Use of Saturable Reactors as Discharge Devices," IEE Proceedings (London), Part 3: Radio and Communication, vol. 98, p. 185, 1951.

[7] D. L. Birx, E. J. Lauer, L. L. Reginato, J. Schmidt, and M. Smith, Basic Principles Governing the Design of Magnetic Switches, Lawrence Livermore National Laboratory, Livermore Calif., UCID 18831 (1980).

[8] W. C. Nunnally, Magnetic Switches and Circuits, Los Alamos National Laboratory, Los Alamos, New Mexico, LA--8862-MS (Revised), 1982.